AIAA 81-0264R

A d^2-Law for Multicomponent Droplet Vaporization and Combustion

C. K. Law* and H. K. Law†
Northwestern University, Evanston, Ill.

The multicomponent analog of the classical spherically symmetric single-component d^2-Law for droplet vaporization and combustion has been formulated based on the concept that the extremely slow rate of liquid-phase mass diffusion causes the droplet concentration distributions to attain almost constant values during much of the droplet lifetime. Explicit formulas are presented allowing direct evaluation of all properties of interest. Experimental results obtained for an alcohol-alkane binary droplet confirm the d^2-Law behavior and the compositional dependence of the burning rate constant. The characteristics of internal bubbling leading to disruptive combustion are also discussed.

Nomenclature

C = specific heat at constant pressure
d_s = droplet diameter
$\mathfrak{D}$ = mass diffusivity
H = heat needed for droplet heating for unit mass of liquid gasified
K = burning rate constant, $-\mathrm{d}(d_s^2)/\mathrm{d}t$
$\bar{K}$ = normalized burning rate constant, Eq. (37)
L_i = specific heat of vaporization
$\tilde{L}$ = $\Sigma\epsilon_i L_i$
Le = Lewis number, $\lambda/(C\rho\mathfrak{D})$
m_i = mass burning rate
$\hat{m}_F$ = $m_F/(4\pi\rho_g\mathfrak{D}_g r_s)$
p = pressure
Q_i = specific heat of combustion
$\tilde{Q}$ = $\Sigma\epsilon_i Q_i$
r = radial distance
$\tilde{r}_f$ = r_f/r_s
R_i = gas constant
T = temperature
$\hat{T}$ = $C_g T$
T_L = limit of superheat
W_i = molecular weight
X_i = molar fraction
Y_i = mass fraction
$\tilde{Y}_{0\infty}$ = $Y_{0\infty}/\Sigma\epsilon_i\nu_i$
β_i = L_i/R_i
γ = $(\lambda_g C_\ell)/(\lambda_\ell C_g)$
ϵ_i = $m_i/m_F = m_i/\Sigma m_i$
η = $\gamma m_F Le_\ell(1-\sigma)$
λ = thermal conductivity coefficient
ν_i = stoichiometric oxidizer to fuel mass ratio
ρ = density
σ = r/r_s
τ = transformed time
χ = defined in Eq. (7)

Subscripts

b = boiling state
f = flame
F = all the vaporizing fuel species
g = gas phase
i = index for vaporizing species
ℓ = liquid phase
n = normal atmosphere
O = oxidizer
s = droplet surface
0 = initial state
∞ = ambiance
$1,2$ = inner and outer regions to the flame

Presented as Paper 81-0264 at the AIAA 19th Aerospace Sciences Meeting, St. Louis, Mo., Jan. 12-14, 1981; submitted Feb. 3, 1981; revision received Sept. 8, 1981. Copyright © American Institute of Aeronautics and Astronautics, Inc., 1981. All rights reserved.

*Professor, Department of Mechanical and Nuclear Engineering. Member AIAA.

†Senior Scientific System Analyst, Department of Mechanical and Nuclear Engineering.

I. Introduction

RECENT concern over the wide-specification nature of synthetic and derived fuels has generated much interest in the vaporization and combustion of multicomponent liquid fuel droplets,[1,2] which frequently determine the bulk combustion characteristics of sprays in many forms of liquid-fueled combustors. Compared with the conventional petroleum fuels, these fuel blends have more complex compositions and also wider and higher boiling point ranges. It is then obvious that not only the fuel vaporization process, but also such strongly kinetically-dependent gas-phase combustion phenomena as ignition, extinction, and pollutant formation will depend sensitively on the composition of the liquid fuel and how its vaporization is modeled. The classical d^2-Law model for droplet vaporization and combustion,[3,4] which is formulated for a single-component fuel but has been used for multicomponent fuels, is not expected to be adequate to meet the more stringent demands just mentioned.

The basic spherically-symmetric model for multicomponent droplet vaporization and combustion has been formulated in Ref. 5. The model assumes equilibrium vaporization at the droplet surface, flame-sheet combustion, and the heat and mass transport processes being transient-diffusive in the liquid phase and quasisteady, convective-diffusive in the gas phase. Only numerical solution of the governing equations was attempted[5] because although explicit expressions can be obtained for all of the gas-phase properties of interest, they are expressed in terms of the interfacial parameters which depend on the liquid-phase processes. These processes are governed by heat-conduction type equations with a moving boundary, viz., the regressing droplet surface, which are only amenable to numerical solutions. The numerical efforts are further complicated by the stiffness of the coupled governing equations because of the much faster thermal diffusion rate compared with the mass diffusion rate. Thus, there is the need for approximate analytical solutions describing multicomponent droplet vaporization and combustion.

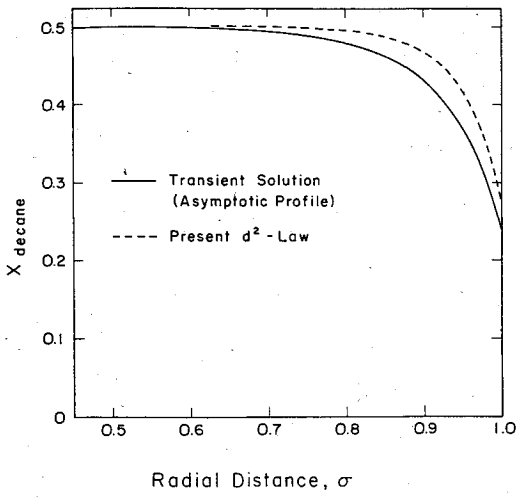

Fig. 1 Comparison of the nearly-asymptotic concentration profile from the numerical transient solution with the quasisteady profile of the present multicomponent d^2-Law.

The numerical results of Ref. 5 do yield the following interesting observation. Because of the slow rate of liquid-phase mass diffusion compared with those of thermal diffusion and surface regression, the liquid-phase concentrations rapidly approach almost constant profiles after vaporization is initiated. The concentrations vary steeply close to the surface, but rapidly approach their initial values when moving inward. This behavior is illustrated in Fig. 1, which shows the molar fractions vs the normalized radial distance, for a 50-50 molar-% of decane-dodecane droplet undergoing vaporization in a 2000 K, 1 atm environment. The rate with which the concentrations attain their constant profiles is actually limited by, and therefore follows, the rate of droplet heating, to be discussed next.

Our previous studies on droplet heating[6,7] have shown that after initiation of vaporization, the surface layer is heated rapidly to attain almost its steady-state temperature; during this period vaporization is slow because most of the heat arriving at the droplet surface is used for droplet heating. However, once this massive surface layer, which contains much of the droplet mass, is heated up, vaporization will proceed at a fast rate because the subsequent heating of the much lighter inner core demands only small amounts from the overall heat budget at the surface. These results demonstrate that significant droplet heating and rapid vaporization are somewhat mutually exclusive events, and that after the initial period the droplet surface can be considered to be at its steady-state value such that droplet heating is almost negligible as far as the heat requirement is concerned. Furthermore, since the droplet concentration profiles closely follow the temperature variations at the droplet surface, they attain their steady-state values whenever the droplet surface has reached its steady-state temperature. In particular, when there is only little droplet heating, which is likely to be the practical situation of interest because only a sufficiently hot droplet is ignitable, the droplet concentrations will attain their steady-state profiles fairly early in the droplet lifetime.

Based on the preceding discussions, a quasisteady model has been formulated and is presented herein. The governing equations are stated and solved in the next section. In Sec. III results from an experiment involving spherically-symmetric droplet combustion are presented; they substantiate the basic mechanisms of the theoretical model. Finally, limitation and utility of the model, particularly the further exploration of a disruptive combustion phenomena caused by internal superheating,[5] are discussed.

II. Theoretical Model

The situation of interest is the isobaric, spherically symmetric vaporization of a droplet, initially of radius r_{s0}, temperature $T_0(r)$, and consisting of N miscible compounds characterized by their respective mass fractions $Y_{i0}(r)$, molecular weights W_i, specific latent heats of vaporization L_i, normal boiling temperatures T_{bni} evaluated at the normal atmospheric pressure p_n, that at time $t=0$ is introduced, and ignited in the case of combustion, in a stagnant, unbounded atmosphere. The atmosphere is characterized by its temperature T_∞, pressure p_∞, and mass fractions $Y_{0\infty}$ of an oxidizing gas O and $(1-Y_{0\infty})$ of a noncondensable inert gas, say nitrogen.

Assuming[4] gas-phase quasisteadiness, flame-sheet combustion, and conventional transport properties including unitary Lewis number, it can be shown[5] that the total and fractional mass vaporization rate, m_F and $\epsilon_i = m_i/m_F$, the flame-front location $\hat{r}_f$, the flame temperature T_f, and H can all be expressed in terms of the states at the droplet surface,

$$\hat{m}_F = \ell n\left\{1 + \frac{\hat{T}_\infty - \hat{T}_s + \tilde{Y}_{0\infty}\tilde{Q}}{\tilde{L}+H}\right\} \tag{1}$$

$$\epsilon_i = Y_{igs}/Y_{Fgs} \tag{2}$$

$$\hat{r}_f = \frac{\hat{m}_F}{\ell n(1+\tilde{Y}_{0\infty})} \tag{3}$$

$$\hat{T}_f = \frac{\hat{T}_\infty - \tilde{Y}_{0\infty}(\tilde{L}+H-\tilde{Q}-\hat{T}_s)}{1+\tilde{Y}_{0\infty}} \tag{4}$$

and

$$H = \frac{(\hat{T}_\infty - \hat{T}_s + \tilde{L} + \tilde{Y}_{0\infty}\tilde{Q})(1-Y_{Fgs}) - \tilde{L}(1+\tilde{Y}_{0\infty})}{\tilde{Y}_{0\infty}+Y_{Fgs}} \tag{5}$$

In the preceding we also have $\hat{m}_F = m_F/(4\pi\rho_g \mathcal{D}_g r_s)$, $\hat{T} = C_g T$, $\tilde{L} = \Sigma\epsilon_i L_i$, $\tilde{Q} = \Sigma\epsilon_i Q_i$, $\tilde{Y}_{0\infty} = Y_{0\infty}/\Sigma\epsilon_i\nu_i$, where ν_i is the stoichiometric oxidizer-to-fuel mass ratio, and the summation is to be performed over all of the vaporizing species F. The problem has also been formulated in such a generalized manner that the results specialize to pure vaporization simply by setting $Y_{0\infty}=0$. For pure vaporization in an environment consisting of some of the vaporizing species such that $Y_{i\infty}\neq 0$, then Eq. (2) is modified[5] and some of the following derivations are also somewhat more algebraically cumbersome. We choose not to include this special case for the sake of simplicity and clarity.

Evaluation of the quantities in Eqs. (1-5) requires knowledge of the temperature T_s and fuel vapor concentration $Y_{Fgs} = \Sigma Y_{igs}$ at the droplet surface. If we assume for simplicity ideal mixture behavior and equilibrium vaporization, then the vapor concentrations can be expressed through Raoult's law

$$X_{igs} = X_{i\ell s}\chi_i(T_s) \tag{6}$$

where $\chi_i(T_s)$ is the equilibrium molar concentration for the pure component i. The functional form of $\chi_i(T_s)$ depends on the particular relation used to calculate the vapor pressure; for example if we use the Clausius-Clapeyron relation, then

$$\chi_i(T_s) = \left(\frac{p_n}{p_\infty}\right)\exp\left\{\beta_i\left(\frac{1}{T_{bni}} - \frac{1}{T_s}\right)\right\} \tag{7}$$

where $\beta_i = L_i/R_i$ and R_i is the gas constant. It may also be emphasized that the ideal mixture assumption is not essential toward development of the model. Realistic behavior of nonideal mixtures can be incorporated through the use of activity coefficients.

Using Eqs. (6) and (7), it is seen that the quantities in Eqs. (1-5) now depend on T_s and $X_{i\ell s}$, which are to be determined by studying the liquid-phase transport processes. Indeed, the primary objective of the present analysis is to determine these two quantities. Hence, according to earlier discussion, we shall assume that the droplet surface temperature and its concentration distributions remain constant at T_s and $Y_{i\ell}(r)$, respectively. The temperature assumption implies that it is not necessary to study liquid-phase heat conduction. Furthermore, since there is very little droplet heating, Eq. (5) is simply

$$H(Y_{Fgs}, T_s) = 0 \tag{8}$$

which gives an independent relation between Y_{Fgs} and T_s.

To obtain the concentration distributions according to our assumption, we first write the general transient-diffusion equation[5]

$$\frac{\partial Y_{i\ell}}{\partial t} = \frac{\mathfrak{D}_\ell}{r^2}\frac{\partial}{\partial r}\left(r^2\frac{\partial Y_{i\ell}}{\partial r}\right) \tag{9}$$

Since the droplet surface is continuously regressing, the location of one of the liquid-phase boundaries is time dependent. It is, however, advantageous to include all the transient effects in the differential equation such that the boundary conditions are time independent. Thus with the new independent variables

$$\sigma = \frac{r}{r_s(t)} \quad \text{and} \quad \tau = \int_0^t \frac{(\lambda_\ell/C_\ell\rho_\ell)}{r_s^2(t')}dt'$$

Eq. (9) is transformed to

$$\frac{\partial Y_{i\ell}}{\partial \tau} = \frac{1}{Le_\ell\sigma^2}\frac{\partial}{\partial\sigma}\left(\sigma^2\frac{\partial Y_{i\ell}}{\partial\sigma}\right) - \gamma\hat{m}_F\sigma\frac{\partial Y_{i\ell}}{\partial\sigma} \tag{10}$$

with the initial and boundary conditions[5]

$$Y_{i\ell}(\sigma, 0) = Y_{i\ell 0}(\sigma) \tag{11}$$

$$(\partial Y_{i\ell}/\partial\sigma)_{\sigma=0} = 0 \tag{12}$$

$$(\partial Y_{i\ell}/\partial\sigma)_{\sigma=1} = Le_\ell\gamma\hat{m}_F(Y_{i\ell s} - \epsilon_i) \tag{13}$$

where $\gamma = (\lambda_g C_\ell)/(\lambda_\ell C_g)$, $Le_\ell = \lambda_\ell/(C_\ell\rho_\ell\mathfrak{D}_\ell)$ is the liquid-phase Lewis number, and the identity $\hat{m}_F = -(\rho_\ell C_g/2\lambda_g)dr_s^2/dt$ has also been used. Thus the liquid boundaries are now fixed at $\sigma = (0,1)$, with the additional convection term in Eq. (10) representing surface regression.

Thus to derive the constant concentration profiles, we set $\partial Y_{i\ell}/\partial\tau = 0$ in Eq. (10), yielding

$$\frac{1}{\sigma^2}\frac{d}{d\sigma}\left(\sigma^2\frac{dY_{i\ell}}{d\sigma}\right) = Le_\ell\gamma m_F\sigma\frac{dY_{i\ell}}{d\sigma} \tag{14}$$

The region of interest here is $\sigma \to 1$, where $Y_{i\ell}$ changes rapidly within a narrow layer. Furthermore, due to diffusional resistance, we also expect that the larger the Le_ℓ, the narrower this layer is. Thus the structure of this layer can be resolved in the stretched coordinate

$$\eta = \gamma\hat{m}_F Le_\ell(1-\sigma) \tag{15}$$

in which the dependence on γ and $\hat{m}_F$ is also included.

Substituting Eq. (15) into Eqs. (14) and (13), we have

$$\frac{d^2Y_{i\ell}}{d\eta^2} = -\frac{dY_{i\ell}}{d\eta} \tag{16}$$

and

$$\left(\frac{dY_{i\ell}}{d\eta}\right)_{\eta=0} = -(Y_{i\ell s} - \epsilon_i) \tag{17}$$

The second boundary condition for Eq. (16) is

$$(Y_{i\ell})_{\eta\to\infty} = Y_{i\ell 0} \tag{18}$$

which implies that the droplet interior remains uninfluenced.

The solution of Eqs. (16-18) is

$$Y_{i\ell} = Y_{i\ell 0} + (Y_{i\ell s} - \epsilon_i)\exp\{-\gamma\hat{m}_F Le_\ell(1-\sigma)\} \tag{19}$$

which displays the structure of the concentration profile. Since, generally, $\gamma = 0(1)$ and $\hat{m}_F = 0(1)$ except for very slow rates of vaporization, the exponential term is significant only for regions close to the droplet surface where $(1-\sigma) = 0(Le_\ell^{-1})$.

Equation (19) is still not explicit because of $Y_{i\ell s}$ and ϵ_i. Evaluating Eq. (19) at the droplet surface, $\sigma = 1$, we obtain

$$\epsilon_i = Y_{i\ell 0} \tag{20}$$

which states that the fractional mass vaporization rate is equal to the initial mass fraction. This result is consistent with the overall mass conservation and the present quasisteady assumption, as should be.

Thus equating Eqs. (2) and (20), and using Eq. (6), we have

$$Y_{i\ell 0} = \frac{Y_{igs}}{\Sigma Y_{jgs}} = \frac{X_{igs}W_i}{\Sigma X_{jgs}W_j} = \frac{X_{i\ell s}W_i\chi_i}{\Sigma X_{j\ell s}W_j\chi_j} = \frac{Y_{i\ell s}\chi_i}{\Sigma Y_{j\ell s}\chi_j} \tag{21}$$

which yields

$$Y_{i\ell s} = (Y_{i\ell 0}/\chi_i)(\Sigma Y_{j\ell s}\chi_j) \tag{22}$$

Summing over Eq. (22),

$$(\Sigma Y_{i\ell 0}/\chi_i)(\Sigma Y_{i\ell s}\chi_i) = 1 \tag{23}$$

Using Eqs. (22) and (23), we finally obtain

$$Y_{i\ell s} = \frac{Y_{i\ell 0}/\chi_i}{\Sigma Y_{j\ell 0}/\chi_j} \tag{24}$$

and

$$Y_{i\ell}(\sigma; T_s) = Y_{i\ell 0}\left\{1 + \left[\frac{1/\chi_i}{\Sigma Y_{j\ell 0}/\chi_j} - 1\right]\exp[-\gamma\hat{m}_F Le_\ell(1-\sigma)]\right\} \tag{25}$$

Equation (25) is the final expression for the concentration profile $Y_{i\ell}$. The only unknown parameter here is T_s, which is needed to determine $\hat{m}_F$ and χ_i.

The droplet temperature T_s can be found by solving Eq. (8), in which Y_{Fgs} can be expressed by first combining Eqs. (2) and (20),

$$Y_{Fgs} = Y_{igs}/Y_{i\ell 0} \tag{26}$$

Converting Y_{igs} to X_{igs}, using Eq. (6) to relate X_{igs} to $X_{i\ell s}$, converting $X_{i\ell s}$ back to $Y_{i\ell s}$, and then using Eq. (24) to relate $Y_{i\ell s}$ to $Y_{i\ell 0}$, it can be shown that Eq. (26) can be expressed as

$$Y_{Fgs} = \left\{1 + W_A\left[\Sigma\left(\frac{Y_{i\ell 0}}{W_i}\right)\left(\frac{1}{\chi_i} - 1\right)\right]\right\}^{-1} \tag{27}$$

where W_A is an average molecular weight of all the non-vaporizing species at the droplet surface. In arriving at Eq.

(27) one also may note the care needed in the conversion between the molar and mass fractions. This is because even though constant molecular weight has been assumed in the gas-phase solutions, molecular weight effect is much stronger, especially for the case of pure vaporization, in evaluating the vapor pressures at the droplet surface and therefore should be properly accounted.

The problem is completely solved at this stage. Thus, once T_s is determined from Eq. (8) using Eq. (27), $\hat{m}_F$ and $Y_{it}(\sigma)$ are, respectively, given by Eqs. (1) and (25). The instantaneous droplet size then follows the d^2-Law behavior

$$d_s^2 = d_{s0}^2 - Kt \tag{28}$$

where $K = (8\lambda_g / C_g \rho_{\ell s})\hat{m}_F$ and

$$\tilde{\rho}_{\ell s} = (\Sigma Y_{i\ell s}/\rho_{\ell i})^{-1} = (\Sigma Y_{i\ell 0}/\chi_i)/(\Sigma Y_{i\ell 0}/\chi_i \rho_{\ell i})$$

It is of interest to compare the evaporation rate constant K derived herein

$$K = \frac{8\lambda_g}{C_g\{(\Sigma Y_{i\ell 0}/\chi_i)/(\Sigma Y_{i\ell 0}/\chi_i\rho_{\ell i})\}} \times \ell n\left\{1 + \frac{C_g(T_\infty - T_s) + (Y_{0\infty}/\Sigma Y_{i\ell 0}\nu_i)(\Sigma Y_{i\ell 0} Q_i)}{(\Sigma Y_{i\ell 0} L_i)}\right\} \tag{29}$$

with the formula intuitively stated by Wood et al.[8]

$$K = \frac{8\lambda_g}{C_g\{\Sigma Y_{i\ell 0}\rho_{\ell i}\}} \ell n\left\{1 + \frac{C_g(T_\infty - T_s) + (Y_{0\infty}/\nu)(Q)}{(\Sigma Y_{i\ell 0} L_i)}\right\} \tag{30}$$

It is seen that Eq. (30) uses a single ν and Q, without properly weighing the contributions from different species. The average density also is expressed incorrectly. Finally, there is also no provision in Ref. 8 for the calculation of T_s, which is an important quantity for pure vaporization.

Next, we note that in deriving Eqs. (1-5), and subsequently Eq. (29), we have assumed constant transport properties and frozen equilibrium at the flame. It is generally recognized that while these assumptions may not affect the qualitative trend of the combustion behavior, they do cause serious uncertainty and inaccuracy in quantitative predictions. The situation is particularly serious for combustion in an oxidizer-rich environment in that the high flame temperature not only assures the importance of product dissociation, it also causes greater variation and, thereby, uncertainty in estimating the average transport property values.

To approximately allow for these effects, we have derived an improved expression for the burning rate constant,

$$K = \frac{8\lambda_{g1}}{C_{g1}\rho_{\ell s}} \ell n\left[1 + \frac{C_{g1}(T_f - T_s)}{\Sigma Y_{i\ell 0} L_i}\right] + \frac{(\rho_g \mathcal{D}_g)_2}{\lambda_{g1}/C_{g1}} \ell n\left[1 + \frac{Y_{0\infty}}{\Sigma Y_{i\ell 0}\nu_i}\right] \tag{31}$$

In Eq. (31) we have allowed for constant, but unequal values for λ_g, C_g, and $(\rho_g \mathcal{D}_g)$ for both the inner and outer regions to the flame, where the subscripts *1* and *2*, respectively, designate the inner and outer regions. it is also expressed in terms of the flame temperature T_f, which is simply the adiabatic flame temperature assuming (concentration-weighted) stoichiometric composition and dissociation equilibrium. Thus, it can be separately evaluated using standard chemical equilibrium calculations.[9] Determination of the average transport coefficients requires proper concentration weighting and using the ⅓ rule for temperature averaging. Details and justifications of this approach can be found in Ref. 10. Equation (31) is the expression we actually used in comparison with our experimental data, as will be discussed later.

It is also significant to note that the solution procedure of the present multicomponent d^2-Law is of the same degree of simplicity as the classical single-component d^2-Law; namely, it involves an iterative determination of T_s followed by straightforward substitution for other quantities. The single-component case, however, does offer one possibility of further simplification. That is, when the droplet is vaporizing vigorously, for all practical purposes T_s can be approximated by the liquid boiling point under prevailing pressure, which is a given fuel property. On the other hand, the boiling point for the multicomponent fuel still has to be iteratively determined by solving Eq. (27) with $Y_{Fgs} = 1$, or

$$\Sigma\left(\frac{Y_{i\ell 0}}{W_i}\right)\left(\frac{1}{\chi_i(T_b)} - 1\right) = 0 \tag{32}$$

An approximate analytical expression can be derived from Eq. (32) for T_b. If we use Eq. (7) for χ_i and if T_{bi} is the boiling point of the ith species at p_∞, then χ_i can also be expressed as

$$\chi_i = \exp\left\{\beta_i\left(\frac{1}{T_{bi}} - \frac{1}{T_b}\right)\right\} \tag{33}$$

For mixture components with close boiling points, Eq. (33) can be expanded, yielding

$$\chi_i \simeq 1 + \beta_i\left(\frac{1}{T_{bi}} - \frac{1}{T_b}\right) \tag{34}$$

Substituting Eq. (34) into Eq. (32) and rearranging, we obtain

$$T_b \simeq \frac{\Sigma X_{i\ell 0}\beta_i}{\Sigma X_{i\ell 0}\beta_i / T_{bi}} \tag{35}$$

Equation (35) is most useful for $p_\infty = 1$ atm because the T_{bi}'s are tabulated values. Furthermore, since for most liquids $\beta_i / T_{bi} \simeq$ const at normal atmosphere according to Trouton's rule, Eq. (35) becomes

$$T_b \simeq \Sigma X_{i\ell 0} T_{bi} \tag{36}$$

which simply states that the boiling point of the mixture is the sum of the molar-concentration-weighted boiling points of the individual components. The result is reasonable.

For a burning droplet an accurate knowledge of T_s actually is not essential in determining $\hat{m}_F$ because of the dominance of the chemical heat release, $\tilde{Y}_{0\infty}\tilde{Q}$, over the sensible heat $C_g(T_\infty - T_s)$. The dependence on T_s is somewhat stronger for K because of its influence on the liquid density $\tilde{\rho}_{\ell s}$. At any rate, it is reasonable to expect that quite accurate estimates for all of the bulk combustion parameters can be obtained through simple substitution by using Eq. (36). In the case of pure vaporization, however, an accurate knowledge of T_s, obtained through iteration, may be necessary.

To demonstrate the salient features of the model, Fig. 1 compares the nearly asymptotic (at half-life) concentration profile of the transient numerical solution of Ref. 5 with the quasisteady profile of the present d^2-Law. The property values used are $C_g = 1$ cal/g-K, $\gamma = 0.2$, and $Le_\ell = 30$. It is seen that the comparison is quite satisfactory. The predicted droplet temperature of 458 K also agrees closely with the asymptotic value of 460 K from the numerical solution.

Figure 2 shows the compositional variations of the normalized burning rate constant

$$\tilde{K} = \frac{K - K_{\text{octanol}}}{K_{\text{undecane}} - K_{\text{octanol}}} \tag{37}$$

for an octanol/undecane droplet burning in an environment characterized by $T_\infty = 300$ K, $p_\infty = 90$-mm Hg, and

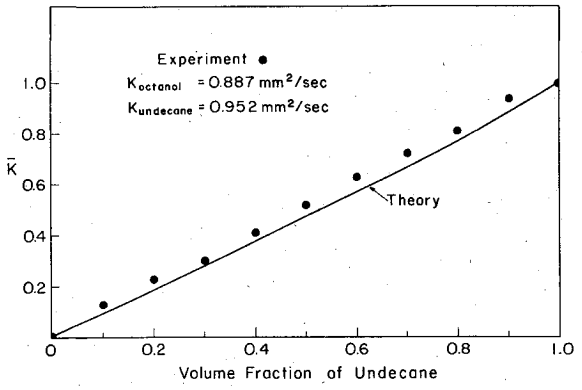

Fig. 2 Dependence of the theoretical and experimental values of the normalized burning rate constant on the mixture composition for an octanol-undecane droplet.

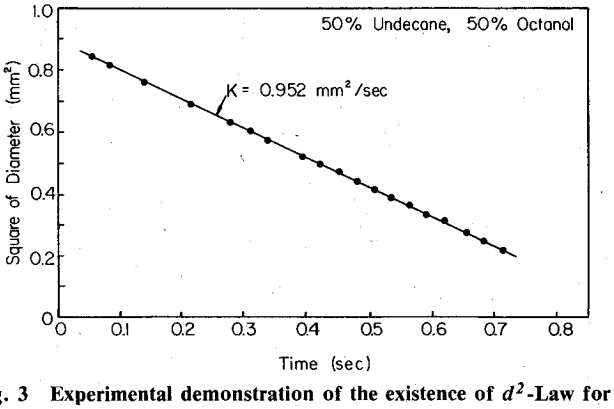

Fig. 3 Experimental demonstration of the existence of d^2-Law for multicomponent droplets.

$X_{0\infty} = 0.40$. This is the system adopted for our experimental investigation, as will be discussed later. Equation (31) is used in generating the results in Fig. 2. Thus, it is seen that $\bar{K}$, and therefore $\hat{m}_F$, vary with the volume fraction in a somewhat linear fashion. It is further found that this variation primarily is due to the higher latent heat of vaporization of octanol relative to undecane; the difference in the chemical heat release is small. It is obvious that the compositional variation of $\hat{m}_F$ can be either widened by using a lower alcohol (say ethanol instead of octanol), or narrowed by substituting octanol by another alkane such that both components have similar heats of vaporization and combustion.

III. Experimental Investigation

For an experimental investigation of the present multicomponent droplet combustion model, we have adopted the suspended droplet, spark-ignition technique for its simplicity and controllability. However, several considerations are needed in order for the experiment to conform with the basic features of the model, as will be explained in the following.

Perhaps the most important feature of the model is that liquid-phase mass transport is diffusion controlled, implying the absence of any internal recirculatory motion which is frequently generated by external convection, either forced or natural. Thus, for the suspended droplet experiment it is essential to either eliminate or minimize buoyancy. Our approach to achieve this is to conduct the experiment under low pressure. To compensate for any possible finite-rate kinetic effects which degrade the flame-sheet assumption, the environment is, in addition, enriched with oxygen. We have thus determined that an environment with $p_\infty = 90$-mm Hg and $X_{0\infty} = 0.40$ satisfies the requirements.[11] Other details of the experimental apparatus and procedure can be found in Ref. 11.

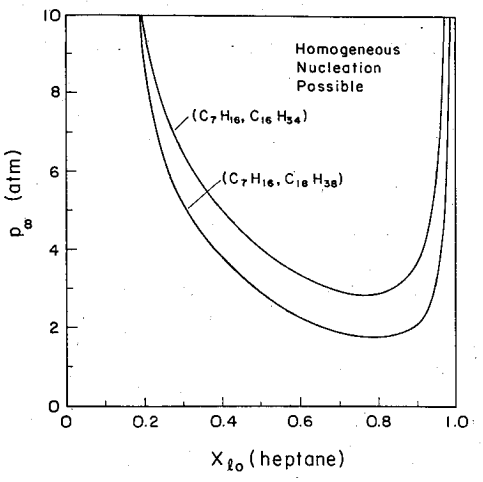

Fig. 4 Compositional dependence of the onset of internal homogeneous nucleation.

The binary components selected for study are octanol and *n*-undecane, which have almost the same boiling points at 1 atm. The need to approximately match the boiling points of the components arises from the potential occurrence of internal bubbling if the components have substantially different boiling points. The particular volatility selected is a compromise between minimizing the extent of prevaporization before ignition such that there is negligible change in the droplet composition from the prepared value, and minimizing the amount of droplet heating as required by the model.

Figure 3 shows variation of the square of the droplet diameter with time for a binary-component droplet initially consisting of 50% undecane and 50% octanol by volume. The droplet heating period, which spans about 10-15% of the droplet lifetime, is not shown here because of the relatively large scatter caused by ignition disturbance. Figure 3 demonstrates conclusively that d_s^2 varies linearly with time and is, therefore, in agreement with the quasisteady, spherically-symmetric liquid-phase diffusion controlled combustion described by the model. This behavior is qualitatively different from that observed by Wood et al.,[8] who reported that their d^2 vs t curve exhibits a finite curvature with the initial and final slopes corresponding to those of the more or less volatile components, respectively. While the reported close agreement seems somewhat surprising considering possible influence due to initial transient droplet heat up and also the accuracy of the raw data, the qualitative trend does substantiate the concept that in their experiments liquid-phase mass transfer is facilitated through the buoyancy-generated internal circulation, such that the volatility differentials exert stronger influence on the burning behavior. For sprays under practical situations, the droplet sizes are much smaller. Hence, the intensities of both natural and forced convection are relatively weaker, implying that the present diffusion-controlled combustion mode may be the dominant one under suitable situations.

In Fig. 2 the experimental data for $\bar{K}$ is compared with the theoretical curve, where $K_{\text{octanol}} = 0.887$ mm²/s and $K_{\text{undecane}} = 0.952$ mm²/s. It is clear that while the theoretical curve predicts well the experimental data, for mixtures the predictions are consistently slightly less than the observed values. This may be caused by the ideal mixture assumption used in the theory. Since octanol and undecane obviously cannot form an ideal mixture because of their difference in the molecular structures, it is reasonable to expect that the fuel vapor pressure at the droplet surface is slightly higher than that given by Raoult's law. This can cause the observed slightly higher burning rate.

IV. Discussions on Internal Bubbling

The knowledge of the droplet concentration profile allows direct estimation of the importance of such liquid-phase kinetic processes as carbonization and internal boiling and superheating.[5] The possibility of internal bubbling caused by the nucleation of the more volatile components, which are prevented from reaching the droplet surface because of diffusional resistance, was first theoretically demonstrated to be possible by Landis and Mills[12] for heterogeneous nucleation, and by Law[5] for homogeneous nucleation. This event may enhance significantly fuel spray atomization. Using the present simplified formulation, and assuming as a limiting case that the droplet temperature is uniform at T_s, the possible occurrence of internal bubbling can be assessed easily by checking if the relations

$$T_s > \Sigma X_{i\ell}(\sigma)\, T_{Li} \quad \text{for homogeneous nucleation} \tag{38}$$

or

$$T_s > T_h(\sigma; X_{i\ell}) \quad \text{for heterogeneous nucleation} \tag{39}$$

are satisfied, where T_{Li} is the limit of superheat[5,13] and T_h is the boiling point corresponding to the local mixture composition. Figure 4 shows the dependence of homogeneous nucleation on pressure and composition for a burning binary droplet, with $T_\infty = 300$ K and $Y_{0\infty} = 0.23$. It is seen that increasing the pressure enhances nucleation because the droplet can then sustain a higher temperature due to the elevation of the boiling point. The nucleation boundary exhibits a parabola-like profile, as originally observed in Ref. 14. It is also in qualitative agreement with the recent experimental results of Ref. 15. For these curves nucleation is favored for an optimum mix of the high- and low-boiling-point fuels; the high-boiling-point fuel is needed to drive up the droplet temperature because of its high concentration at the surface, whereas the low-boiling-point fuel is needed to facilitate nucleation in the droplet interior. Thus, widening the boiling point difference, say by substituting hexadecane with octadecane, enhances the occurrence of nucleation. It may also be emphasized that the boundaries shown in Fig. 4 were obtained by using the thermodynamic limit of superheat as the criterion. In experimental situations homogeneous nucleation may occur before this limit. Then the boundaries in Fig. 4 will be shifted downward.

V. Concluding Remarks

In the present study we have derived a simplified, approximate, solution for the quasisteady, spherically-symmetric, liquid-phase mass diffusion controlled vaporization and combustion of multicomponent fuel droplets. This solution allows direct evaluation of all combustion properties of interest, including the liquid-phase composition profiles, once the droplet surface temperature is determined iteratively. Therefore, utilization of the present multicomponent d^2-Law is almost as simple as the classical pure-component d^2-Law.

It is, however, worth emphasizing the limitations of the present model. It is not applicable during the initial period of droplet burning when the initial droplet temperature and concentration profiles are adjusting to their quasisteady values. It also breaks down for small values of Le_ℓ and excessively slow rate of vaporization, when $\hat{m}_F Le_\ell < 0(1)$. For these cases the problem has to be treated as transient. The model also ceases to be useful as internal circulation generated by external convection becomes intense. The bulk combustion behavior can then be assessed using either an approximate, batch-distillation type model[16] or a more rigorous, two-dimensional model recently formulated by Lara-Urbanejo and Sirignano.[17]

Acknowledgments

The theoretical and experimental phases of this research were, respectively, sponsored by the Division of Basic Energy Sciences, Department of Energy, under Contract DE-AC02-77ER04433, and by the Heat Transfer Program of the National Science Foundation under Grant CME-7820013. We also thank S. H. Chung, K. Miyasaka, and C. J. Park for their assistance with this problem.

References

[1] Sirignano, W. A. and Law, C. K., "Transient Heating and Liquid-Phase Mass Diffusion in Droplet Vaporization," *Advances in Chemistry Series*, No. 166, edited by J. T. Zung, American Chemistry Society, Washington, D.C., 1978, pp. 1-26.

[2] Faeth, G. M., "Current Status of Droplet and Liquid Combustion," *Progress in Energy Combustion Science*, Vol. 3, 1977, pp. 191-224.

[3] Godsave, G.A.E., "Studies of the Combustion of Drops in Fuel Spray: The Burning of Single Drops of Fuel," *Fourth Symposium (International) on Combustion*, Williams and Wilkins, Baltimore, Md., 1953, pp. 818-830.

[4] Williams, F. A., *Combustion Theory*, Addison-Wesley, Reading, Mass., 1964.

[5] Law, C. K., "Internal Boiling and Superheating in Vaporizing Multicomponent Droplets," *AIChE Journal*, Vol. 24, 1978, pp. 626-632.

[6] Law, C. K. and Sirignano, W. A., "Unsteady Droplet Combustion with Droplet Heating—II: Conduction Limit," *Combustion and Flame*, Vol. 28, 1977, pp. 175-186.

[7] Law, C. K., "Unsteady Droplet Combustion with Droplet Heating," *Combustion and Flame*, Vol. 26, 1976, pp. 17-22.

[8] Wood, B. J., Wise, H., and Inami, S. H., "Heterogeneous Combustion of Multicomponent Fuels," *Combustion and Flame*, Vol. 4, 1960, pp. 235-242.

[9] Penner, S. S., *Chemistry Problems in Jet Propulsion*, Pergamon Press, New York, 1957.

[10] Chung, S. H. and Law, C. K., "A Simplified Theory for Droplet Combustion with Dissociation," to be published.

[11] Miyasaka, K. and Law, C. K., "Combustion of Strongly-Interacting Linear Droplet Arrays," *Eighteenth Symposium (International) on Combustion*, Combustion Institute, Pittsburgh, Pa., 1981, pp. 283-292.

[12] Landis, R. B. and Mills, A. F., "Effects of Internal Diffusional Resistance on the Vaporization of Multicomponent Droplets," Fifth International Heat Transfer Conference, Paper B7.9, Tokyo, Japan, 1974.

[13] Blander, M. and Katz, J. L., "Bubble Nucleation in Liquids," *AIChE Journal*, Vol. 21, 1975, pp. 833-848.

[14] Law, C. K., Law, H. K., and Lee, C. H., "Combustion Characteristics of Coal/Oil and Coal/Oil/Water Mixtures," *Energy*, Vol. 4, 1979, pp. 329-339.

[15] Lasheras, J. C., Fernandez-Pello, A. C., and Dryer, F. L., "On the Disruptive Burning of Free Droplets of Alcohol/n-Paraffin Mixtures and Emulsions," *Eighteenth Symposium (International) on Combustion*, Combustion Institute, Pittsburgh, Pa., 1981, pp. 293-305.

[16] Law, C. K., "Multicomponent Droplet Combustion with Rapid Internal Mixing," *Combustion and Flame*, Vol. 26, 1976, pp. 219-233.

[17] Lara-Urbanejo, P. and Sirignano, W. A., "Theory of Transient Multicomponent Droplet Vaporization in a Convective Field," *Eighteenth Symposium (International) on Combustion*, Combustion Institute, Pittsburgh, Pa., 1981, pp. 1365-1374.